PAPER Special Section on Metamaterials for Microwave and Millimeter-Wave Applications

Modal Analysis of Finite-Thickness Slab with Single-Negative Tensor Material Parameters

Masashi HOTTA[†a)], **Mitsuo HANO**[†], ***Members***, ***and*** **Ikuo AWAI**[††], ***Fellow***

SUMMARY Eigenvalue equations and expressions of EM fields for volume modes in an anisotropic single-negative slab with tensor material parameters is presented. By the comparison with the eigenvalue equation of surface modes along single-negative slab with negative scalar permeability, the validity of the present study is confirmed. We have also made clear which elements of the material parameter tensors affect existence of TE and TM modes in the slab. Taking the dispersion of material parameters into consideration, we demonstrate in detail that TE modes propagate in a slab with one negative element of the permeability tensor numerically. These TE modes turn out to be the magnetostatic waves (MSWs), which is the first demonstration of the MSW in a nonmagnetic material.

key words: *metamaterial, anisotropy, single-negative material, tensor material parameter, magnetostatic wave*

1. Introduction

Metamaterials with negative permeability and/or permittivity have attracted much interest due to their extraordinary electromagnetic (EM) characteristics [1]–[10]. The artificially fabricated metamaterial can be classified with combination of the positive and negative signs of material parameters into four categories. Most ordinary category includes the double-positive material with all positive material parameters in which the right-handed waves propagate. The other categories are the double-negative material with all negative material parameters and the single-negative materials with either permeability or permittivity negative. It has been taken for granted that the wave can propagate only in the double-positive and double-negative materials but can not propagate in the single-negative materials. There have been known, however, some exceptions, such as surface plasmon [11], impedance surface wave [12] and magnetostatic surface wave (MSSW), which propagate along the interface of single-negative and double-positive materials [2]–[5]. The present authors reexamined those waves in the light of the sign of material parameters. They demonstrated under what circumstances TE or TM surface modes can propagate along the boundary of semi-infinite and finite-thickness slab with single-negative material whose permittivity and permeability are both scalar but one of them is negative [6].

It should also be noted that the single-negative material is intrinsically anisotropic. Typical metamaterial with negative permeability or permittivity can be realized by stacking sheet of substrate with printed split-ring resonators (SRRs) on their surface [7] or embedded thin metal wires [8], [9]. These structures exhibit a negative material constant only to one direction. In fact, three sets of perpendicular stacks of substrate are required to realize isotropic structures as shown in Ref. [7]. Thus, it will be more realistic to analyze the anisotropic structure that has tensor material parameters.

In this paper, to clarify the effect of the anisotropy of the single-negative material and find their new application, we have presented the wave equations of TE and TM modes in the material with permeability and permittivity tensors whose components are allowed to take negative or positive values according to the directions, and also derived the eigenvalue equations together with the EM field of volume modes in finite-thickness single-negative slab structure.

Secondly, solving the TE mode eigenvalue equation of the finite-thickness slab with negative permeability tensor numerically, we have presented the dispersion characteristics of the propagation constant and field distributions for those volume modes. The electric and magnetic energies are compared for this TE mode, resulting in the overwhelming dominance of the latter. This fact suggests that this mode could be a magnetostatic wave (MSW).

In the last, the magnetostatic approximation is applied to the present structure and it is found to support MSWs. In addition, by ignoring the term $\omega^2\varepsilon_0\mu_0$ compared with β^2 in the dispersion relation for the TE mode, we will arrive at the MSW dispersion relation, and hence, the TE mode in a single-negative slab will be proved to be an MSW again.

2. Basic Structure and Field Expressions

2.1 Finite-Thickness Slab with Negative Tensor Material Parameters

As shown in Fig. 1, we analyze the TE and TM modes in finite-thickness slab with tensor permittivity $\hat{\varepsilon}$ and permeability $\hat{\mu}$ whose components are allowed to be negative and the slab thickness is T (region II). The coordinate system used in the analysis is also shown in the same figure. It is assumed that the tensor permittivity and tensor permeability of slab are linear and simultaneously diagonalizable,

$$\hat{\varepsilon} = \begin{pmatrix} \varepsilon_x & 0 & 0 \\ 0 & \varepsilon_y & 0 \\ 0 & 0 & \varepsilon_z \end{pmatrix}, \quad \hat{\mu} = \begin{pmatrix} \mu_x & 0 & 0 \\ 0 & \mu_y & 0 \\ 0 & 0 & \mu_z \end{pmatrix} \qquad (1)$$

Manuscript received January 10, 2006.

Manuscript revised April 3, 2006.

[†]The authors are with the Graduate School of Science and Engineering, Yamaguchi University, Ube-shi, 755-8611 Japan.

[††]The author is with the Department of Electronics and Informatics, Ryukoku University, Otsu-shi, 520-2194 Japan.

a) E-mail: hotta@yamaguchi-u.ac.jp

DOI: 10.1093/ietele/e89–c.9.1283

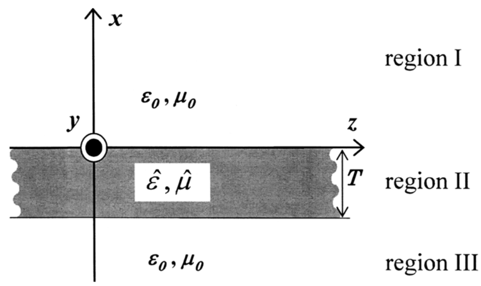

Fig. 1 Finite-thickness slab with permittivity and permeability tensor.

The upper and lower regions of the slab are the free-space with the material parameters ε_0 and μ_0 (regions I and III).

2.2 Field Expression and Eigenvalue

To get the eigen solutions and the corresponding eigenvalues, we start from the following source-free Maxwell's equations,

$$\nabla \times \mathbf{H} = j\omega\hat{\varepsilon}\mathbf{E}, \quad \nabla \times \mathbf{E} = -j\omega\hat{\mu}\mathbf{H} \tag{2}$$

where $\hat{\varepsilon}$ and $\hat{\mu}$ are the permittivity and permeability tensors defined by Eq. (1), respectively, and time and z-dependence of the EM fields is assumed as $\exp\{j(\omega t - \beta z)\}$. Furthermore, the structure for the analysis has no variation toward the y-direction, and hence, the partial differential operators as to y and z can be replaced as follows,

$$\frac{\partial}{\partial y} \Rightarrow 0, \quad \frac{\partial}{\partial z} \Rightarrow -j\beta. \tag{3}$$

Then, the Maxwell's Eq. (2) in region II are decomposed into the following set of equations,

$$\begin{cases} j\beta H_y = j\omega\varepsilon_x E_x & \text{(4a)} \\ -j\beta H_x - \dfrac{\partial H_z}{\partial x} = j\omega\varepsilon_y E_y & \text{(4b)} \\ \dfrac{\partial H_y}{\partial x} = j\omega\varepsilon_z E_z & \text{(4c)} \\ j\beta E_y = -j\omega\mu_x H_x & \text{(4d)} \\ -j\beta E_x - \dfrac{\partial E_z}{\partial x} = -j\omega\mu_y H_y & \text{(4e)} \\ \dfrac{\partial E_y}{\partial x} = -j\omega\mu_z H_z . & \text{(4f)} \end{cases}$$

2.2.1 TE Mode

By choosing Eqs. (4b), (4d), and (4f), we can get the wave equation for TE volume mode in region II as

$$\frac{\partial^2 H_z}{\partial x^2} + \delta_1^2 H_z = 0, \tag{5}$$

where

$$\delta_1 = \sqrt{\frac{\mu_z}{\mu_x}\left(\omega^2\varepsilon_y\mu_x - \beta^2\right)} . \tag{6}$$

In the same manner, we can also derive the wave equation in regions I and III, as follows,

$$\frac{\partial^2 H_z}{\partial x^2} - \delta_0^2 H_z = 0 \qquad \text{with } \delta_0 = \sqrt{\beta^2 - \omega^2\varepsilon_0\mu_0} . \tag{7}$$

Solving the wave equations in each region, respectively, we can get the field expressions for TE mode in the following.

For region I ($x \geq 0$) and III ($x \leq -T$), from Eqs. (7), (4d), and (4f) with the boundary condition at $x = \pm\infty$, each field component can be expressed as follows.

For region I($x \geq 0$),

$$H_z = C_1 e^{-\delta_0 x}, \quad H_x = -\frac{j\beta C_1}{\delta_0} e^{-\delta_0 x}, \quad E_y = \frac{j\omega\mu_0 C_1}{\delta_0} e^{-\delta_0 x} \tag{8}$$

and, for region III($x \leq -T$),

$$H_z = D_1 e^{\delta_0 x}, \quad H_x = \frac{j\beta D_1}{\delta_0} e^{\delta_0 x}, \quad E_y = -\frac{j\omega\mu_0 D_1}{\delta_0} e^{\delta_0 x} \tag{9}$$

where C_1 and D_1 are arbitrary constants.

Next, for region II ($-T \leq x \leq 0$), we can obtain the following field components from Eqs. (5), (4d), and (4f), considering that the expected solutions for the volume modes have sinusoidal variation inside the slab.

$$\begin{cases} H_z = A_1 \cos\delta_1 x + B_1 \sin\delta_1 x \\ H_x = -\dfrac{j\mu_z\beta}{\mu_x\delta_1}(-A_1 \sin\delta_1 x + B_1 \cos\delta_1 x) \\ E_y = \dfrac{j\omega\mu_z}{\delta_1}(-A_1 \sin\delta_1 x + B_1 \cos\delta_1 x) \end{cases} \tag{10}$$

where A_1 and B_1 are arbitrary constants.

Application of the boundary conditions at $x = 0$ and $x = -T$ surfaces for transverse electric and magnetic fields H_z and E_y lead us to the eigenvalue equation,

$$\left(\mu_0^2\delta_1^2 - \mu_z^2\delta_0^2\right)\sin\delta_1 T = 2\mu_0\mu_z\delta_0\delta_1\cos\delta_1 T \tag{11}$$

with

$$\begin{aligned} &A_1 = C_1, \qquad B_1 = \frac{\mu_0\delta_1}{\mu_z\delta_0} C_1, \\ &D_1 = (A_1\cos\delta_1 T - B_1 \sin\delta_1 T)\, e^{\delta_0 T}. \end{aligned} \tag{12}$$

The eigenvalue equation can be decomposed for the modes with even- and odd-symmetry, respectively,

$$\begin{cases} \mu_0\delta_1 \cos\dfrac{\delta_1 T}{2} = -\mu_z\delta_0 \sin\dfrac{\delta_1 T}{2} & \textit{even mode,} \\ \mu_0\delta_1 \sin\dfrac{\delta_1 T}{2} = \mu_z\delta_0 \cos\dfrac{\delta_1 T}{2} & \textit{odd mode.} \end{cases} \tag{13}$$

In this paper, we have used the terms '*even mode*' and '*odd mode*' to express the symmetry of dominant field component, that is, the longitudinal magnetic field, H_z, for TE mode.

Furthermore, to confirm the validity of the eigenvalue equation (11), we transform it to that of TE surface mode presented as Eq. (10) of Ref. [6]. In order to express the single-negative sheet with negative scalar permeability and positive scalar permittivity, we set the components of the permittivity and the permeability tensors as,

$$\varepsilon_x = \varepsilon_y = \varepsilon_z = \varepsilon_1, \tag{14}$$

$$\mu_x = \mu_z = -\mu_1, \tag{15}$$

where ε_1 and μ_1 are the positive real quantities. When the components of material parameters are set as Eqs. (14) and (15), the phase constant δ_1 in Eq. (6) becomes imaginary,

$$\delta_1 = j\sqrt{\omega^2\varepsilon_1\mu_1 + \beta^2} = j\delta_1', \tag{16}$$

where δ_1' is real quantity.

By substituting Eq. (16) into the eigenvalue equation (11) and using Euler's relation, we can get the same eigenvalue equation for TE surface mode appeared in Eq. (10) of Ref. [6].

Note that the y-component of the permeability tensor is not included in the analysis above. This means that TE mode can propagate along the slab waveguide, regardless of the y-component. When μ_z is negative, while μ_x is positive, like

$$\mu_x = -\mu_z = \mu_1. \tag{17}$$

Equation (6) becomes

$$\delta_1 = j\sqrt{\omega^2\varepsilon_1\mu_1 - \beta^2} = j\delta_1'', \tag{18}$$

as long as ε_1 and μ_1 are larger than ε_0 and μ_0, respectively, δ_1'' can be a real quantity, and hence, the EM field should constitute a surface mode.

Now, we summarize the relationship between the sign of permeability tensor components and the modes propagating to the z-direction in the slab extending to y- and z-directions as shown in Fig. 1.

Table 1 shows 4 types of modes three of which were described in this section. The last one(type d) is similar to conventional volume mode that propagates in a dielectric slab waveguide, except that negative μ_y is allowed as a result of extension to metamaterials. The other 3 types exist in a slab of anisotropic negative permeability.

2.2.2 TM Mode

In the case of TM modes, by selecting Eqs. (4a), (4c), and (4e), we obtain the wave equation in region II as

Table 1 Existence of TE modes in slab shown in Fig. 1 with possible sign combinations of permeability tensor, where all components of permittivity tensor are assumed as positive quantities.

	μ_x	μ_y	μ_z	δ_1	
a)	+	±	−	Imag.	TE surface mode
b)	−	±	−	Imag.	TE surface mode
c)	−	±	+	Real	TE volume mode
d)	+	±	+	Real	Conventional TE volume mode

$$\frac{\partial^2 E_z}{\partial x^2} + \delta_2^2 E_z = 0, \tag{19}$$

where

$$\delta_2 = \sqrt{\frac{\varepsilon_z}{\varepsilon_x}\left(\omega^2\varepsilon_x\mu_y - \beta^2\right)}\ . \tag{20}$$

In the regions I and III, we can also find the same equation as that of TE mode Eq. (7) with proper interchange of the magnetic and electric components. Then, convergence of each field component at $x = \pm\infty$ gives the following expressions.

For region I ($x \geq 0$),

$$E_z = C_2 e^{-\delta_0 x}, \quad E_x = \frac{j\beta C_2}{\delta_0}e^{-\delta_0 x}, \quad H_y = \frac{j\omega\varepsilon_0 C_2}{\delta_0}e^{-\delta_0 x} \tag{21}$$

and for region III ($x \leq -T$),

$$E_z = D_2 e^{\delta_0 x}, \quad E_x = \frac{j\beta D_2}{\delta_0}e^{\delta_0 x}, \quad H_y = \frac{j\omega\varepsilon_0 D_2}{\delta_0}e^{\delta_0 x} \tag{22}$$

where C_2 and D_2 are arbitrary constants.

For region II ($-T \leq x \leq 0$), from Eq. (19), EM fields of TM mode inside the slab can be written as,

$$\begin{cases} E_z &= A_2\cos\delta_2 x + B_2\sin\delta_2 x \\ E_x &= -\dfrac{j\varepsilon_z\beta}{\varepsilon_x\delta_2}(-A_2\sin\delta_2 x + B_2\cos\delta_2 x) \\ H_y &= -\dfrac{j\omega\varepsilon_z}{\delta_2}(-A_2\sin\delta_2 x + B_2\cos\delta_2 x). \end{cases} \tag{23}$$

Applying the boundary conditions at $x = 0$ and $x = -T$ surfaces for transverse electric and magnetic fields E_z and H_y, we can get the following eigenvalue equation

$$\left(\varepsilon_0^2\delta_2^2 - \varepsilon_z^2\delta_0^2\right)\sin\delta_2 T = 2\varepsilon_0\varepsilon_z\delta_0\delta_2\cos\delta_2 T \tag{24}$$

with

$$\begin{aligned} &A_2 = C_2,\ B_2 = \frac{\varepsilon_0\delta_2}{\varepsilon_z\delta_0}C_2, \\ &D_2 = (A_2\cos\delta_2 T - B_2\sin\delta_2 T)\,e^{\delta_0 T}. \end{aligned} \tag{25}$$

In the same manner as for TE mode, Eq. (24) can be decomposed into the even- and odd-mode equations, respectively,

$$\begin{cases} \varepsilon_0\delta_2\cos\dfrac{\delta_2 T}{2} = -\varepsilon_z\delta_0\sin\dfrac{\delta_2 T}{2} & \textit{even mode,} \\ \varepsilon_0\delta_2\sin\dfrac{\delta_2 T}{2} = \varepsilon_z\delta_0\cos\dfrac{\delta_2 T}{2} & \textit{odd mode.} \end{cases} \tag{26}$$

Carrying out the same process as those for TE mode, Eq. (24) can be transformed into the eigenvalue equation of TM surface mode with negative scalar permittivity and positive scalar permeability [6] by setting $\varepsilon_x = \varepsilon_z = -\varepsilon_1$ and $\mu_x = \mu_y = \mu_z = \mu_1$ where ε_1 and μ_1 are positive real. In this case, the y-component of permittivity tensor ε_y also does not affect the existence of TM surface mode. It is extended to TM mode in the slab waveguide in general. The TM mode can propagate along the slab waveguide, regardless of the y-component.

3. Numerical Analysis for TE Volume Modes with Negative Permeability Tensor

Solving Eq. (11) numerically, we can obtain the eigenvalues for the TE volume modes. Prior to the numerical calculation, let us consider the combination of positive and negative sign of the permeability tensor which give the volume mode.

Negative permeability material has at least one or more negative components of permeability tensor. To support the TE volume mode in a negative permeability slab, the phase constant δ_1 in Eq. (11) must take a real value, that is, the argument of square root of Eq. (6) must be positive real, then $\mu_x < 0$ and $\mu_z > 0$ is a possible combination of the components for single-negative permeability material. Hence, we set the components of material parameter tensors as follows,

$$\hat{\varepsilon}=\begin{pmatrix} \varepsilon_x & 0 & 0 \\ 0 & \varepsilon_0 & 0 \\ 0 & 0 & \varepsilon_0 \end{pmatrix}, \quad \hat{\mu}=\begin{pmatrix} \mu_x & 0 & 0 \\ 0 & \mu_0 & 0 \\ 0 & 0 & \mu_0 \end{pmatrix}, \tag{27}$$

where $\varepsilon_x = \varepsilon_r(\omega)\varepsilon_0$ and $\mu_x = \mu_r(\omega)\mu_0$, and $\varepsilon_r(\omega)$ and $\mu_r(\omega)$ are the dispersive relative permittivity and permeability. As a numerical example, we have used the frequency dependence of the following relative permeability for SRRs (Split-Ring-Resonators) expressed in Eq. (43) of Ref. [7],

$$\mu_r(\omega) = 1 - \frac{\dfrac{\pi r^2}{a^2}}{1 + j\dfrac{2l\sigma_1}{\omega\mu_0 r} - \dfrac{3lc_0^2}{\pi\omega^2 \ln\dfrac{2c}{d} r^3}}, \tag{28}$$

where c_0 is the velocity of light. The other parameters of SRRs used in this paper are chosen to be much smaller than the free-space wavelength as shown in Fig. 2.

Figure 3 shows the dispersion characteristic of the relative permeability Eq. (28) with the resistance of SRRs zero, that is, $\sigma_1 = 0.0$. The dimensions and other structural parameters of SRRs are the same as those in Ref. [7] and the slab thickness is set as $T = 1.0$ mm. In this material, $\mu_r(\omega)$ becomes negative over the range of frequency from the singular point at 13.48 GHz to 14.41 GHz and is also smaller than −1.0 below 13.92 GHz as shown in Fig. 3. It seems that the material with this permeability tensor can be realized by stacking the appropriately printed SRR boards as shown in Fig. 4. It has been pointed out that the relative permittivity of this material has no dispersion and its absolute value is close to unity [7]. Thus the x-component of the permittivity tensor, ε_x, assumed to be ε_0 in the following analysis.

Solving the eigenvalue equation (11), we show the dispersion characteristics of TE_1 to TE_4 volume modes in Fig. 5 together with the odd- and even-symmetry TE surface modes, TE_{os} and TE_{es}, [6] for comparison. From these results, we know that the propagation constants of the TE volume modes go down toward the cutoff frequency 13.92 GHz as increasing the operating frequency. This nature tells us that the obtained TE modes are backward waves, having the same property as the modes in double-negative material. In addition to this backward wave nature of obtained volume modes, Fig. 5 also shows that the surface modes in single-negative slab have forward wave nature. This relationship between obtained volume modes and corresponding surface modes in the single-negative slab is much similar to those of MSW modes and the magnetostatic surface wave (MSSW) mode in ferromagnetic slab [13].

Substituting the eigen values obtained at the operating frequency 13.75 GHz to the field expressions (8)–(10) for each mode, we can get profiles of the longitudinal magnetic field, H_z, and transverse electric field, E_y, as shown in Fig. 6, where the slab region II is indicated by gray coloring.

Furthermore, we estimate the time-average energy stored in the EM field to investigate the nature of these

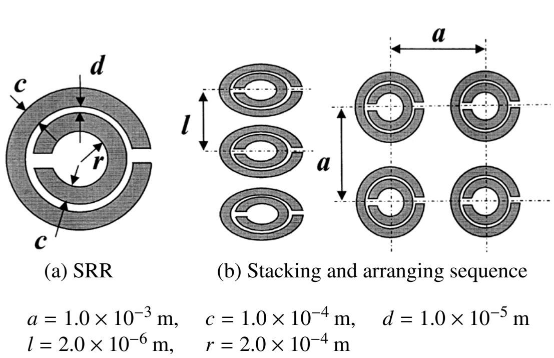

Fig. 2 Dimensions and definition of distances for SRRs [7].

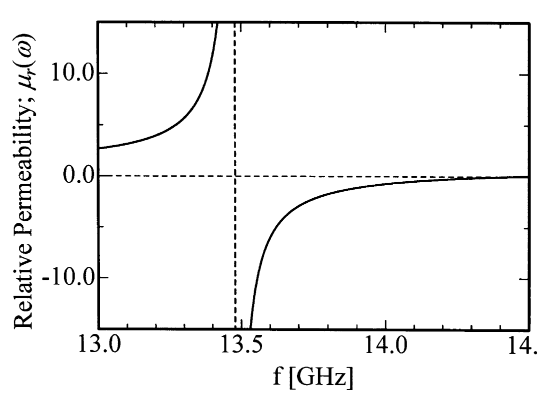

Fig. 3 Dispersive permeability in Ref. [7] with $\sigma_1 = 0.0\,\Omega$.

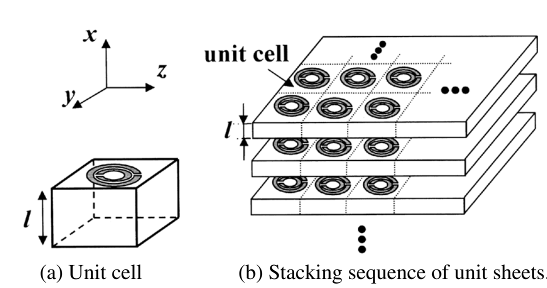

Fig. 4 Structure of metamaterial with negative permeability in x-direction.

modes in more detail. The electric and magnetic stored energy for unit length of the slab waveguide is given, respectively, by the following integral expressions [14].

$$W_e = \frac{\varepsilon_0}{4}\int_{-\infty}^{\infty} \mathbf{E}\cdot\mathbf{E}^* \frac{\partial\{\omega\varepsilon_r(\omega)\}}{\partial\omega}dx, \tag{29}$$

$$W_m = \frac{\mu_0}{4}\int_{-\infty}^{\infty} \mathbf{H}\cdot\mathbf{H}^* \frac{\partial\{\omega\mu_r(\omega)\}}{\partial\omega}dx \tag{30}$$

where $\varepsilon_r(\omega)$ and $\mu_r(\omega)$ are the relative permittivity and permeability with dispersion, respectively. In our analysis, it is assumed that the permittivity of the material has no dispersion but the permeability in the x-direction is dispersive. Substituting the electric and magnetic field expressions in each region (8)–(10) and the expressions for the dispersive permeability Eq. (28) with $\sigma_1 = 0.0$ to Eqs. (29) and (30), we can obtain the energy stored in EM fields of single-negative finite-thickness slab with the negative permeability tensor.

Figure 7 presents the time-average energy stored in the magnetic field as well as the ratio of the electric and magnetic energy for the TE_1 mode. This result tells us that the

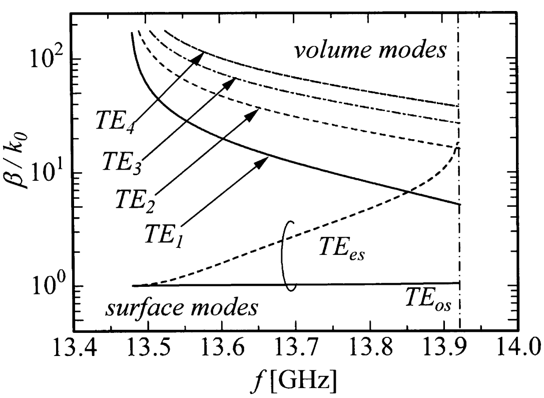

Fig. 5 Dispersion characteristics of the TE volume modes and TE surface waves in the material with negative permeability tensor and positive permittivity tensor.

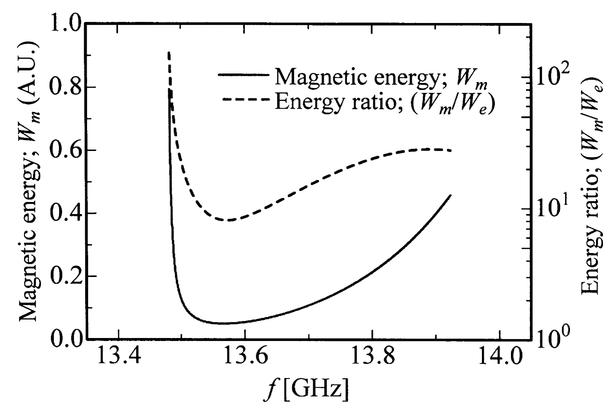

Fig. 7 Electric and magnetic energy of TE_1 mode in dispersive media.

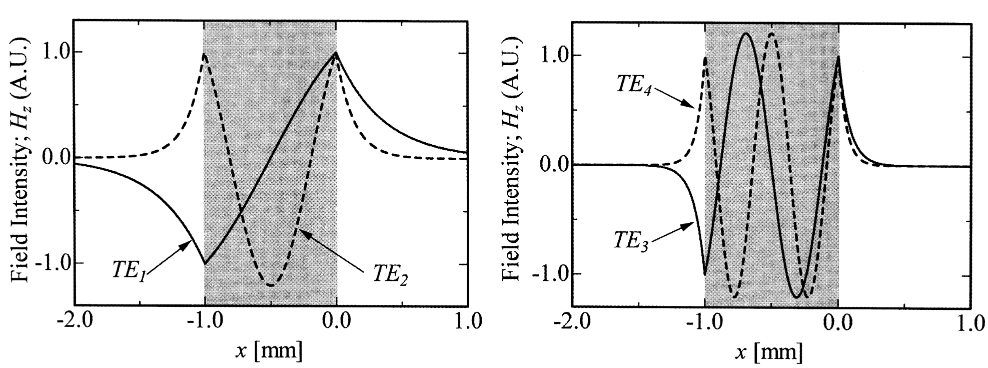

(a) Magnetic field profiles of TE_1, TE_2, TE_3, and TE_4 modes.

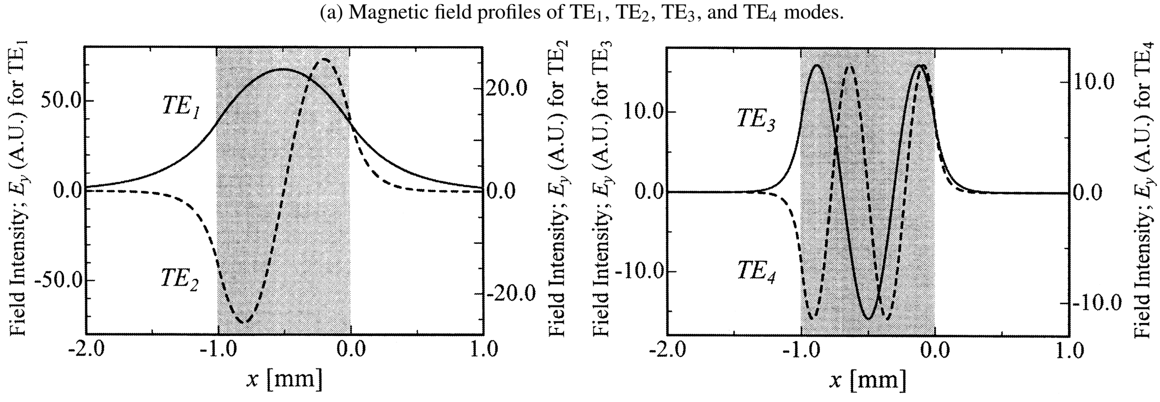

(b) Electric field profiles of TE_1, TE_2, TE_3, and TE_4 modes.

Fig. 6 Electromagnetic field profiles of the volume mode in single-negative slab with tensor material parameters, where $T = 1.0$ mm and $f = 13.75$ GHz. The x-component of permeability tensor μ_x is only negative and dispersive quantity.

energy stored in the magnetic field is extremely larger than the electric counterpart suggesting the possibility that these modes are the magnetostatic waves. In the next section, we will examine it, looking for the solution of the magnetostatic wave equations.

For a slab with negative permittivity tensor, on the other hand, TM mode dispersion relation and field distributions will be easily obtained with proper interchange of the electric and magnetic field components due to the duality of the electric and magnetic fields in the similar manner as Sect. 2.2.2.

4. Magnetostatic Approximation

To verify that volume modes described in the last section are the magnetostatic waves, we will analyze the structure based on the magnetostatic approximation and examine if there is a solution or not. At first, we will assume the same structure as Sect. 3. Then, for the magnetostatic mode, Maxwell's equation in region II can be expressed as follows,

$$\begin{cases} \nabla \times \mathbf{H} = \mathbf{0}, & (31) \\ \nabla \cdot \hat{\mu}\mathbf{H} = 0. & (32) \end{cases}$$

Equation (31) allows $\mathbf{H}$ given by

$$\mathbf{H} = -\nabla\Psi \tag{33}$$

where Ψ is an unknown scalar potential. The following scalar wave equation is derived by substituting Eq. (33) into Eq. (32).

$$\mu_x \frac{\partial^2\Psi}{\partial x^2} + \mu_y \frac{\partial^2\Psi}{\partial y^2} + \mu_z \frac{\partial^2\Psi}{\partial z^2} = 0. \tag{34}$$

Then, by using the operations (3) due to given structure, we can derive the wave equation for the TE magnetostatic mode in region II as,

$$\mu_x \frac{\partial^2\Psi}{\partial x^2} - \beta^2\mu_0\Psi = 0 \tag{35}$$

where $\mu_x = \mu_r(\omega)\mu_0$ is the dispersive x-component of permeability tensor. In the following discussion, it is assumed that the μ_x takes a negative value, since we have treated the single-negative material, and we set as $\mu_x = -\mu_a\mu_0$ where $\mu_a = |\mu_r(\omega)|$ is a positive real quantity.

By solving Eq. (35), the scalar potential can be expressed as,

$$\Psi = \left(A_3 \cos \frac{\beta}{\sqrt{\mu_a}}x + B_3 \sin \frac{\beta}{\sqrt{\mu_a}}x\right) e^{-j\beta z}, \tag{36}$$

in the region II. In the same manner, the scalar potential in region I and III can be written by the following forms,

$$\Psi = C_3 e^{-\alpha x} e^{-j\beta z} \quad \text{region I,} \tag{37}$$

$$\Psi = D_3 e^{\alpha x} e^{-j\beta z} \quad \text{region III.} \tag{38}$$

where A_3, B_3, C_3, and D_3 are the arbitrary constants, and the relation $\alpha = \beta$ holds, since Ψ should satisfy Eq. (35) with μ_x equal to μ_0 in free-space.

The continuity of $H_z = -\frac{\partial\Psi}{\partial z}$ and $B_x = -\mu(x)\frac{\partial\Psi}{\partial x}$ must be applied at $x = 0$ and $x = -T$ as the boundary conditions, where $\mu(x)$ represents μ_0 in regions I and III, and the x-component of permittivity tensor in region II. Applying these boundary conditions, we can obtain the following eigenvalue equations,

$$\cot \frac{\beta T}{2\sqrt{\mu_a}} = -\sqrt{\mu_a} \quad \textit{even mode}, \tag{39}$$

$$\tan \frac{\beta T}{2\sqrt{\mu_a}} = \sqrt{\mu_a} \quad \textit{odd mode}. \tag{40}$$

Equation (39) gives numerically the same dispersion curves as those of TE_2 and TE_4 volume modes in Fig. 5, while Eq. (40) those of TE_1 and TE_3. In fact, the numerical differences are less than 1%. This result demonstrates that the TE volume modes obtained in Sect. 3 are the magnetostatic modes. We know Eq. (11) contains the terms $\omega^2\varepsilon_0\mu_0$ and $\omega^2\varepsilon_y\mu_x$ implicitly by examining Eqs. (6) and (7). In the magnetostatic approximation, neglecting the displacement current is equivalent to assuming

$$\omega^2\varepsilon_0\mu_0,\ \omega^2\varepsilon_y\mu_x \ll \beta^2. \tag{41}$$

Thus, we obtain the approximated relations

$$\delta_0 \approx \beta, \quad \delta_1 \approx \frac{\beta}{\sqrt{\mu_a}} \tag{42}$$

and arrives at Eqs. (39) and (40) by substituting Eq. (42) into Eq. (13). This result verifies that the TE modes in Sect. 2.2.1 are the magnetostatic waves by another means.

For the TM modes, it is easy to obtain the eigenvalue equations using electrostatic approximation by proper interchange of the electric and magnetic field components. And it has been also confirmed that the TM volume modes obtained in this paper are the electrostatic wave.

The magnetostatic and electrostatic waves have been known to propagate only in the magnetized ferrite and plasma, respectively. It has been taken for granted, in other words, that DC magnetic field plays an essential role, giving a nonreciprocal tensor permeability or permittivity. The present result reveals it is not the case.

The negative values of one or more components of the permeability tensor in case of the MSW, for example, are essential for having a solution of the MSW wave equation (34). If μ_x, μ_y, and μ_z are of the same sign, Eq. (35) cannot have a propagating solution. This property reverses the Poynting energy flow inside the slab, as a result, which partly cancels the Poynting energy flow outside the slab. Thus, this reduction of total energy flow S with preservation of large EM energy W results in the reduction of group velocity v_g as is understood by the equation.

$$v_g = \frac{S}{W} = \frac{S}{W_m + W_e}\,. \tag{43}$$

Thus, negative sign of permeability tensor components also explains the slow wave nature of MSW.

In the last, one more comment on the property of MSWs is added. The definition of the magnetic wave is that it has larger magnetic energy than the electric energy, which is different from that of the magnetostatic wave. The definition of the latter is that it obeys the magnetostatic condition, Eq. (31). Magnetostatic waves, however, have always had a larger magnetic energy, as far as the present authors know. It may be because a negative permeability is induced by some kind of resonance, which is accompanied with a strong dispersion. A large value of permeability and its variation around the resonance frequency could result a large magnetic energy. The result shown in Fig. 7 was also brought about by the resonance shown in Fig. 3.

5. Conclusions

The eigenvalue equation and field expressions of TE and TM modes for the finite-thickness slab structure with single-negative tensor material parameters were demonstrated in consideration for dispersion of material parameters. We have revealed that the nature of the existing modes in the single-negative slab, whether surface mode or volume mode, depends on the sign combination of the tensor components of material parameters.

It is also verified that TE and TM modes obtained in this paper are the magnetostatic and electrostatic wave, respectively, by the magnetostatic or electrostatic approximation analysis. Thus, it has been brought to light that the MSW could exist in nonmagnetic materials. This fact would bring us the possibility of novel microwave and millimeter-wave applications such as midget magnetostatic resonator composed of the nonmagnetic single-negative metamaterial utilizing the short effective wavelength nature of MSWs.

References

[1] V.G. Veselago, "The electrodynamics of substances with simultaneously negative values of ε and μ," Soviet Physics Uspekhi, vol.10, no.4, pp.509–514, 1968.
[2] C. Caloz and T. Itoh, Electromagnetic Metamaterials: Transmission Line Theory and Microwave Applications, John Wiley & Sons, 2006.
[3] R.A. Shelby, D.R. Smith, and S. Schults, "Experimental verification of a negative index of refraction," Science, vol.292, no.5514, pp.77–79, 2001.
[4] A. Alu and N. Engheta, "Guided modes in a waveguide filled with a pair of single-negative (SNG), double-negative (DNG), and/or double-positive (DPS) layers," IEEE Trans. Microw. Theory Tech., vol.52, no.1, pp.199–210, Jan. 2004.
[5] A. Alu and N. Engheta, "Pairing an epsilon-negative slab with a mu-negative slab: Resonance, tunneling and transparency," IEEE Trans. Antennas Propag., vol.51, no.10, pp.2558–2571, Oct. 2003.
[6] M. Hotta, M. Hano, and I. Awai, "Surface waves along a boundary of single negative material," IEICE Trans. Electron., vol.E88-C, no.2, pp.275–278, Feb. 2005.
[7] J.B. Pendry, A.J. Holden, D.J. Robbins, and W.J. Stewart, "Magnetism from conductors and enhanced nonlinear phenomena," IEEE Trans. Microw. Theory Tech., vol.47, no.11, pp.2075–2081, Nov. 1999.
[8] J.B. Pendry, A.J. Holden, W.J. Stewart, and I. Youngs, "Extremely low frequency plasmons in metallic meso structure," Phys. Rev. Lett., vol.76, pp.4773–4776, 1996.
[9] J.B. Pendry, A.J. Holden, D.J. Robbins, and W.J. Stewart, "Low frequency plasmons in thin wire structures," J. Phys., Condens. Matter, vol.10, pp.4785–4809, 1998.
[10] D.R. Smith and D. Schuring, "Electromagnetic wave propagation in media with indefinite permittivity and permeability tensors," Phys. Rev. Lett., vol.90, no.7, pp.(077405)1–4, Feb. 2003.
[11] C. Kittel, Introduction to Solid State Physics, 7th ed., John Wiley & Sons, 1995.
[12] R.E. Collin, Field Theory of Guided Waves, 2nd ed., IEEE Press, 1991.
[13] R.W. Damon and J.R. Eshbach, "Magnetostatic modes of a ferromagnet slab," J. Phys. Chem. Solids, vol.19, no.3/4, pp.308–320, 1961.
[14] R.E. Collin, Foundations for Microwave Engineering, 2nd ed., Chap.2, McGraw-Hill, 1992.

Masashi Hotta received the B.E. and M.E. degrees in electronic engineering from Ehime University, Matsuyama, Japan in 1988 and 1990, respectively, and the Dr. Eng. degree from Osaka Prefecture University, Sakai, Japan in 1995. In April 1990, he joined the Department of Electronic Engineering, Ehime University, Matsuyama, Japan as an Assistant Professor of Electrical and Electronic Engineering, where he had been engaged in research and development of optical devices for optical communication. From April 1997 to February 1998, he was a visiting scholar at the University of California, Los Angeles (UCLA), Los Angeles, USA, on leave from Ehime University. Since April 1999, he has been with the Department of Electrical and Electronic Engineering, Yamaguchi University, Ube, Japan, where he is currently an Associate Professor of the Graduate School of Science and Engineering. His current research interests are focused on the microwave applications of metamaterials and design of guided-wave type optical devices. Dr. Hotta is a member of MTT Society and LEOS of IEEE, Optical Society of America (OSA), the International Society for Optical Engineering (SPIE), and American Association for the Advancement of Science (AAAS).

Mitsuo Hano received the B.E. and M.E. degrees in electrical engineering from Yamaguchi University, Ube, Japan, in 1974 and 1976, and Ph.D. degree from Osaka University, Osaka, Japan, in 1984, respectively. From 1976 to 1979, he was a member of the Faculty of Science, Yamaguchi University. Since 1979, he joined the Department of Electrical and Electronics Engineering, Yamaguchi University, Ube, Japan and he is currently a Professor. He has been engaged in research of electromagnetic field computation and its application to electrical and electronic devices. Dr. Hano is a member of IEE, Japan and IEEE.

Ikuo Awai received the B.S. degree in 1963, M.S. degree in 1965 and Ph.D. in 1978, all from Kyoto University, Kyoto, Japan. In 1968, he joined Department of Electronics, Kyoto University, Kyoto, Japan, as a Research Associate, where he was engaged in microwave magnetic waves and integrated optics. From 1984 to 1990, he worked for Uniden Corporation, Tokyo, Japan, developing microwave communication equipments. He joined Yamaguchi University as a Professor in 1990, where he has studied magnetostatic wave devises, dielectric wave-guide components, super conducting devises and artificial dielectric resonators for microwave application. In 2004, he started to work for Ryukoku University as a Professor, being mainly engaged in microwave filters and meta-materials. Dr Awai is a member of MTT Society of IEEE.